# Engineering Manual For the Jammer Effectiveness Model

## Nicholas DeMinco

**PRODUCT DISCLAIMER**

Certain commercial equipment and programs are identified in this report to adequately explain the operation of the program. In no case does such identification imply recommendation or endorsement by the National Telecommunications and Information Administration, nor does it imply that the program or equipment identified is necessarily the best available for this application.

# CONTENTS

# ENGINEERING MANUAL FOR THE JAMMER EFFECTIVENESS MODEL

Nicholas DeMinco[*]

This engineering manual describes a user-friendly and menu-driven computer program called the Jammer Effectiveness Model (JEM). The models used in JEM to analyze the effectiveness of a jammer in jamming a receiver/transmitter pair or network of receivers and transmitters are described. The JEM runs on a personal computer in a Windows environment. The extensive design and analysis capabilities of this program have been previously limited to mainframe computers. This computer model is highly structured and modular in design, which allows for flexibility and expandability for future modifications.

Key words:    jammer; jamming; propagation; communication systems models; electronic warfare; electronic countermeasures

## 1. INTRODUCTION

The Institute for Telecommunication Sciences (ITS) has developed a user-friendly and menu-driven computer program, the Jammer Effectiveness Model (JEM), that runs in Windows 3.1 as a Windows application. The JEM analyzes the effectiveness of a jammer in jamming a receiver/transmitter pair or a network of receivers and transmitters. The extensive design and analysis capabilities available in this model have been previously limited to mainframe computers. The JEM software model is used primarily by the U. S. Army to evaluate electronic warfare scenarios.

ETSEM (EHF Telecommunication System Engineering Model) was the first-generation model developed by ITS to analyze the effectiveness of communication links [1]. ETSEM modeled the cumulative distribution of bit error rate for digital systems; it also modeled the signal-to-noise ratio in the worst voice channel for analog terrestrial line-of-sight (LOS) communication links. ETSEM was limited in its applications and could not be expanded easily to analyze other communication paths or provide different output options. The need for a simple-to-use and easy-to-update computer program that would run on a personal computer in a DOS environment resulted in the development of the Analysis of Microwave Operational Scenarios (AMOS) computer program [2]. The JEM was created by adding the jamming scenario types to AMOS. The resulting JEM became too large to run in DOS and so the JEM was converted to run in a Windows environment.

---

[*] The author is with the Institute for Telecommunication Sciences, National Telecommunications and Information Administration, U.S. Department of Commerce, Boulder, CO 80303-3328

The highly structured JEM allows for flexibility and expandability. The JEM includes a user-created catalog of equipment, ground stations, and aircraft and satellite platforms; the software for creating and maintaining this catalog; a climatological database for much of the world; and the analysis software. The analysis software includes subroutines for use in calculating clear-air attenuation, rain attenuation, multipath attenuation, diffraction, and troposcatter.

In the JEM, data entry is simplified by the use of user-friendly menus and options. Databases are created as a result of this data entry and saved as scenario descriptions. These scenario descriptions completely characterize the communication link or jamming situation. The scenario description includes: ground or airborne station location, equipment characteristics, and climate, terrain, and other pertinent physical factors. Each of the analysis programs within a scenario analyze the case represented by the scenario description data.

The JEM is organized into six scenario types. A scenario type represents either a communication path geometry description or a jamming geometry description. The four scenario types in the communication geometry description are: ground-to-ground, ground-to-satellite, ground-to-aircraft, and aircraft-to-satellite. The two scenario types in the jamming geometry description are: jamming and jammer versus network. The jamming scenario analyzes: received jammer power versus distance, received transmitter power versus distance, jammer footprint, and isopower contours. The jammer versus network scenario analyzes and evaluates the effects of a jammer on up to five communication nodes. For the jamming geometry description, the receiver, transmitter, and jammer platforms can be on the ground or airborne. The jamming and the jammer versus network scenarios are the major features of the JEM for electronic warfare and interference analysis. The other four scenario types are used as an aid in the evaluation and design of microwave communication systems. They allow the user to simulate a wide variety of propagation effects on the system. The user can run several different types of analyses on the data without having to re-enter it. The data can also be edited easily.

The jamming scenarios of the JEM can be used for analysis in the frequency range of 2 MHz to 20 GHz. The 2- to 30-MHz range includes propagation models for both the ground wave and the sky wave. An irregular terrain model for the 20-MHz to 20-GHz frequency range has also been integrated into the JEM model. The terrain irregularity is specified by a delta h factor to indicate terrain roughness over the path. No use is made of terrain files in the program at this time. The remaining four scenario types can evaluate the design of microwave communication systems operating between 1 and 300 GHz.

Section 2 describes each of the two jammer scenario types and provides an overview of what computations they can perform in addition to a description of the physical models involved in each analysis. Section 3 describes all of the original four microwave communication scenario types and the physical analysis models involved in each. Section 4 contains a summary and Section 5 contains recommendations for future work on JEM. Examples of running JEM are contained in another report that describes how to use the JEM [3].

## 2. JAMMING AND JAMMER VERSUS NETWORK SCENARIOS

The jamming scenario and the jammer versus network scenarios represent the major features of the jammer effectiveness model for electronic warfare calculations for frequencies between 2 MHz and 20 GHz.

### 2.1 The Jamming Scenario

The jamming scenario type contains four analyses: jammer footprint, isopower contours, received signal power versus distance, and received jammer power versus distance.

### 2.1.1 The Jammer Footprint

The jammer footprint is a polar plot of the maximum distance from the jammer versus azimuth angle that the jammer can effectively jam a user-specified friendly link distance. Figure 1 is an example of a jammer footprint plot resulting from a JEM analysis. Figure 1 shows three contours corresponding to three receiver-to-transmitter separations of 30, 50, and 70 km. The user can select up to four transmitter-to-receiver separation (friendly-link) distances for the jammer footprint. The program plots up to four contours, one for each of the user-supplied friendly-link distances. In order to communicate, the transmitter/receiver pair must be on or outside of the contour. As the transmitter-to-receiver separation distance is increased, the pair must be further from the jammer to maintain communication.

The jammer location is specified by the latitude, longitude, and altitude. The receiver location will then be specified by the user. A radial distance and azimuth angle based on true North is used to specify receiver position relative to the jammer position. This is the slant range distance used for propagation loss modeling. The transmitter locations based on the receiver location are also supplied by the user. The user is requested to enter up to four separation distances between the receiver and the transmitter. The location of these four positions are along one radial from the receiver. The four radial distances and one angle from the receiver location are used to specify these transmitter locations. Figure 2 shows the relative geometry of the jammer footprint for three receiver-to-transmitter separations. The receiver antenna beam position is pointed directly along this radial line at the transmitters as a default, and the user can change this position. The transmitter antenna beam positions can only be positioned off-axis by one angle at all four separation distances between the receiver and the transmitter. The initial beam position of the transmitter antennas will be with the transmitter antenna beam pointed directly at the receiver.

Next the received power for each of the transmitter/receiver separations is computed. The ratio of received power to receiver sensitivity (the smallest detectable signal in the presence of internal and external noise) is computed to compare to the required signal-to-noise ratio. This determines
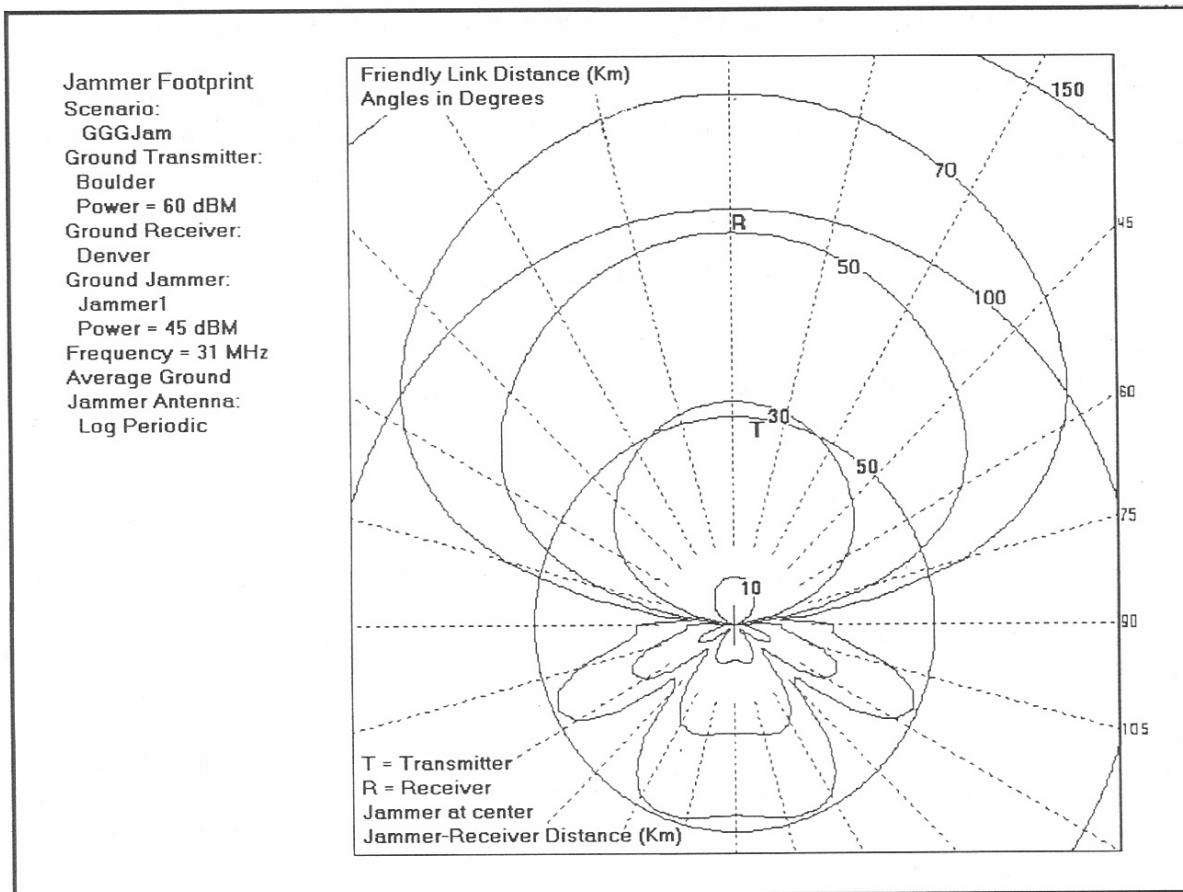
3

**Figure 1. A jammer footprint.**

the possibility of having a good link between these receiver/transmitter pairs. If this condition is not met for any of the transmitter/receiver separations, a message alerts the user and specifies the particular distance or distances at which the condition is not met.

If a link is established, a computation is made to determine what received jammer power level $P_{jr}$ (dBm) is needed to disrupt communications for each transmitter/receiver separation (see Section 2.3.5). This is the minimum received jammer power level needed for a successful jamming condition.

The distance between the jammer and the receiver at which this received jammer power level exists for each transmitter/receiver separation as a function of the azimuth angle about the jammer is then computed. This distance is determined from a table of calculations of received jammer power versus distance and the azimuth angle. This table is created by the computer program. This table is then searched and values interpolated where necessary. If this received jammer power is exceeded for all transmitter/receiver distances, the user is informed of these amounts.
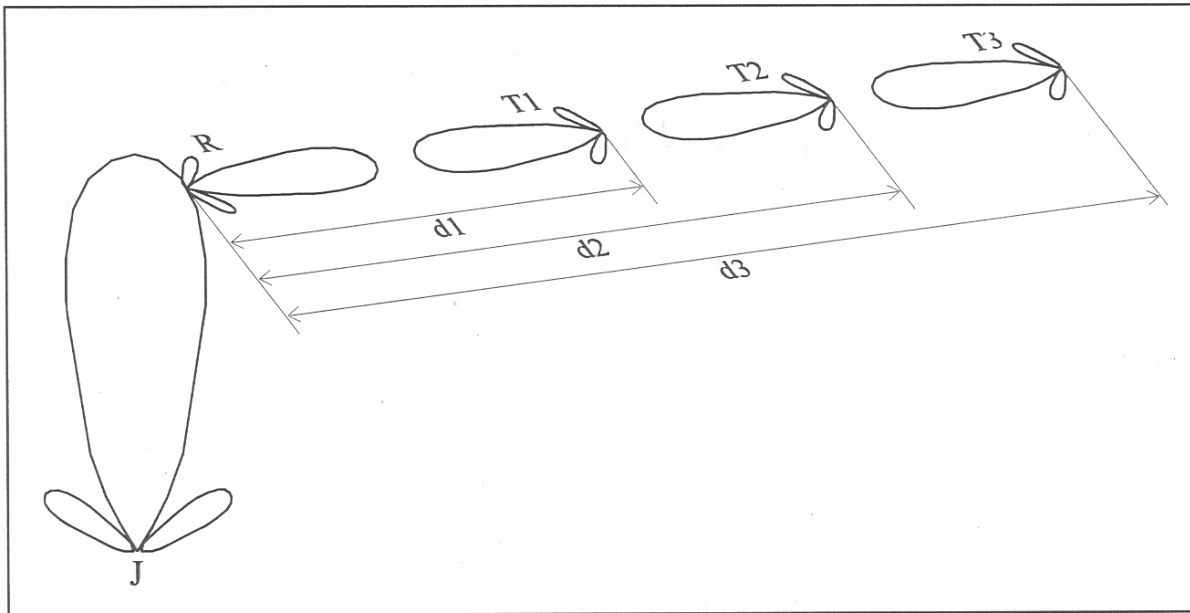
Figure 2.  Geometry of a jammer footprint.

The program performs the computations for the distance necessary to jam the transmitter/receiver pair for the lowest value of $P_{jr}$; this value corresponds to the largest transmitter/receiver pair separation.  This saves overall computation time.  The results are plotted as contours (Figure 1) representing the maximum distance the jammer can disrupt communications for each transmitter/receiver separation versus the azimuth angle about the jammer.

The user is able to steer the jammer beam, the receiver beam, and the transmitter beam. Initially, the receiver beam is pointed directly at the transmitter, and the transmitter beam is pointed directly at the receiver.  The jammer beam is initially pointed at the receiver.  The user may change the beam positions or leave them pointed at each other.  The antenna beam directions are presented as arrows on the display.  The user is presented with a display containing the jammer location (distance and angle based on true North).  The user can also change the locations and re-run the program.

In the jammer footprint analysis, the victim receiver is always a receiver and the transmitter paired with it always operates as a transmitter.  The separation distance between the jammer and receiver is always plotted on the jammer footprint.  The receiver to transmitter separations are indicated on each of the contours.  The four transmitter locations will all be on a straight line at the same angle, but at the different user-selected separation distances.

### 2.1.2 Isopower Contours

The isopower contour is a plot of one or more constant user-specified jammer power density levels at the receiver versus azimuth angle about the jammer.  It determines the distances versus
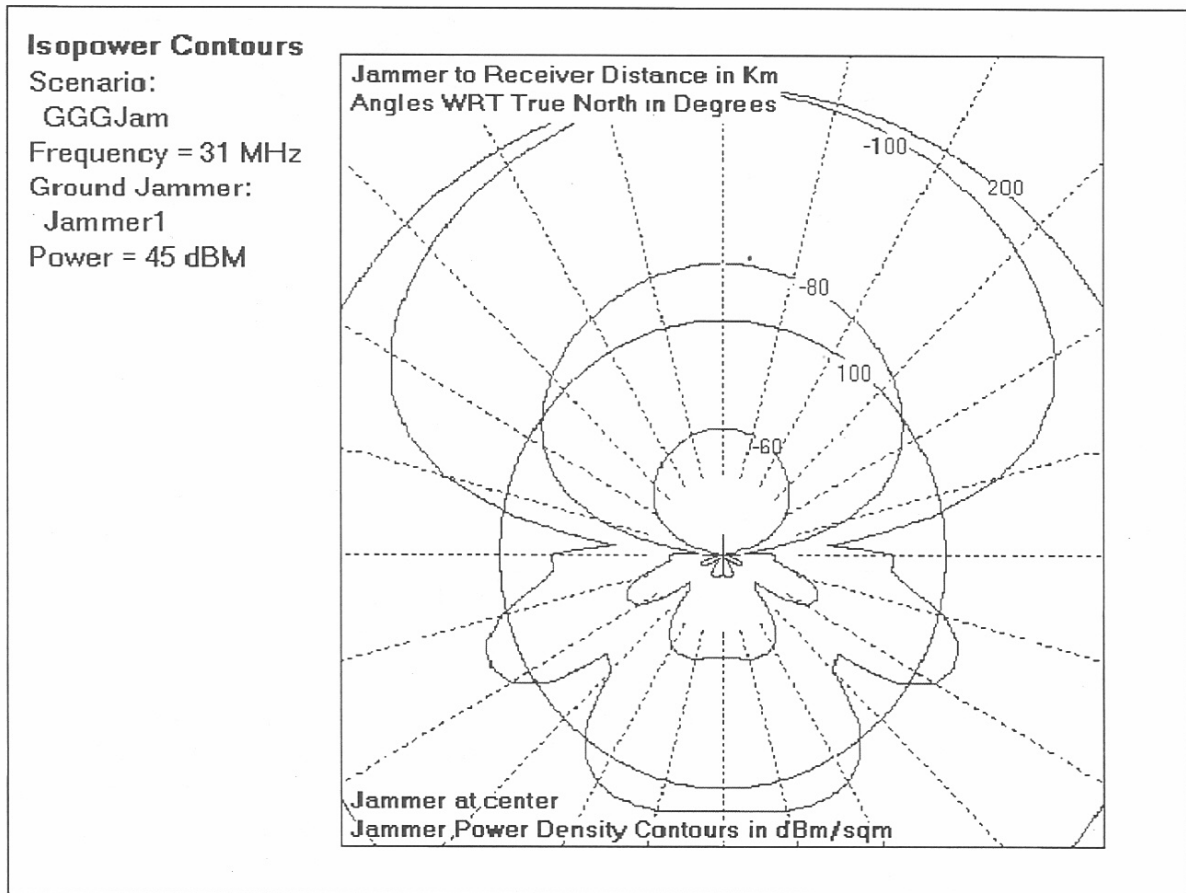
Figure 3. Isopower contour plot.

azimuth angle that the jammer can generate certain discrete power density levels at the receiver location. The user can ask for up to four isopower density contour levels. An example of an isopower contour program output with three power density contours is shown in Figure 3.

The jammer latitude, longitude, and altitude are necessary to provide a reference location for the ionospheric propagation model. Default coordinates will be used for the jammer in the scenario if the user does not supply them. This location can be changed by the user within the analysis.

The equations that are used to compute received signal power density $P_d$ (dBm/m$^2$) received from a jammer for all of the analyses depend on whether the frequency f (MHz) is above or below 30 MHz. If f is less than or equal to 30 MHz, both a ground-wave signal power density level and a sky-wave electric field strength are computed separately and then combined to determine the total signal power density. The electric field strength from the sky-wave model must be converted to a signal power density before combining with the ground-wave component of power density.

If f is greater than 30 MHz, only a ground-wave signal power density is computed using a propagation model that is valid above 30 MHz.

The ground-wave component of the signal power density into the receiver from the jammer $P_{gd}$(dBm/m$^2$) is obtained from

$$P_{gd} = P_j + G_j + 20 \log f - L_j - 38.55 \ ,$$

where

$P_j =$ the jammer power in dBm,

$G_j =$ the jammer antenna gain at the appropriate azimuth angle in dB,

$L_j =$ the ground-wave propagation loss between the jammer and the receiver in dB from either ground-wave model, and

$f =$ the operating frequency in MHz.

The sky-wave electric field strength $E_s$ (dBuV/m) from the jammer is computed using the sky-wave model. The actual addition of the signals is performed after converting this sky-wave electric field strength to the sky-wave component of the signal power density $P_{sd}$(dBm/m$^2$) using:

$$P_{sd} = E_s - 115.76 \ .$$

$P_d$(dBm/m$^2$) is the total jammer power density level into the receiver from combining $P_{gd}$(dBm/m$^2$) and $P_{sd}$(dBm/m$^2$) by addition of their actual power density levels in mW/m$^2$. The power densities must be converted from dBm/m$^2$ to mW/m$^2$ before the addition is performed. The result is then converted back to dBm/m$^2$:

$$P_{gd} \ (dBm/m^2) = 10 \log P_{gd} \ (mW/m^2)$$

$$P_{sd} \ (dBm/m^2) = 10 \log P_{sd} \ (mW/m^2)$$

$$P_d \ (mW/m^2) = P_{gd} \ (mW/m^2) + P_{sd} \ (mW/m^2)$$

$$P_d \ (dBm/m^2) = 10 \log P_d \ (mW/m^2) \ .$$

The dynamic range permitted for the isopower contour levels is computed by determining the maximum and minimum signal power density levels $P_{dmax}$ and $P_{dmin}$. $P_{dmax}$ and $P_{dmin}$ are the received signal power density levels for an azimuth angle of zero degrees (along main beam of jammer) at the distances 0.2 km and 3000 km, respectively, using the computation method above.

This dynamic range is displayed to the user, and the user can supply up to four desired isopower density contour levels $P_{du}$(dBm/sqm) within that range.

The received signal power density from the jammer $P_d$ versus distance can then be computed for any frequency at an azimuth angle of zero degrees, using the computation method described above. The table is then searched at this azimuth angle for the distance at which $P_d$ is equal to one of the values of the desired power density contour level supplied by the user, $P_{du}$ (dBm/m2). These values of azimuth angle, $P_{du}$, and the distance are stored in an array for a table or plotting. The rest of the values of $P_{du}$ are determined while at this azimuth angle and the program stores this angle, $P_{du}$, and the distance for each entry in a look-up table. The lowest isopower contour value and the corresponding distance is used to determine the maximum distance used for computing the rest of the angles in order to reduce computation time.

If the jammer antenna is omnidirectional in azimuth, it is only necessary to compute the power density values at an azimuth angle of zero degrees and use the same value for all radials. The vertical monopole and the vertical log periodic antennas are omnidirectional in azimuth for frequencies less than or equal to 30 MHz. The antennas with frequencies above 30 MHz that are omnidirectional in azimuth include: the vertical monopole, vertical dipole, and discone antennas.

The signal levels will change if the antenna gain changes with azimuthal direction. If the antennas are not omnidirectional in azimuth, $P_d$ is computed for all values of the azimuth angle (0-360 degrees). The azimuth angles, $P_{du}$, and distances are stored in a table for later use for each value of $P_{du}$.

## 2.1.3 Computation of Received Signal Power Level Versus Distance

This analysis module computes the received signal power versus distance from either a transmitter or jammer using the method described in Section 2.3.3. A geographic reference is needed for the ionospheric propagation model, so the user must supply the receiver latitude and longitude. The user must also enter the jammer or transmitter position related to the receiver location using a radial distance and azimuth angle based on true North.

The receiver antenna beam can be positioned from the receiver location, and the jammer or transmitter antenna beam can be positioned from the jammer or the transmitter location (both based on true North). The initial receiver and jammer/transmitter antenna beam positions are directed at each other. The user is shown the beam positions of the receiver and jammer/transmitter antenna. If desired, the user can steer each beam off-axis for each antenna. The appropriate antenna gains are used by the method (see Section 2.3.3). These beam positions are changed by editing entries in Windows. This will change antenna beam angles and allow squinting of beams.

The user enters the initial, final, and incremental distance to use in the computation. The received signal power from the jammer/transmitter versus distance is computed for the frequency of interest.

## 2.2 The Jammer Versus Network Scenario

The jammer versus network scenario is used for evaluating the effects of a jammer on a single transmitter/receiver pair or a network with up to five separate nodes. The scenario can simulate a network and then jam this network with either an airborne or ground-based jammer. The user can move the jammer around to assess the effects of its position.

The user must first enter the location of the network control using latitude, longitude, and altitude. The locations are then entered for up to four receiver/transmitter nodes using radial distances and azimuth angles (based on true North) from the network control location.

The antenna beam positions of the individual nodes, network control, and the jammer can be repositioned by the user. The user can then enter the angles of the receiver/transmitter beam at each node for each link on the graphical beam display of each receiver/transmitter. The user can also position the network control antenna beam on the graphical screen display with an arrow. The jammer beam position is initially pointed at network control and may also be changed via an arrow on the screen display. Further details on beam positioning in the JEM model are contained in [3].                                                                       .

Using the locations for each node, the distances are computed between each pair of nodes for each link. The initial assumption is that a possible link exists between all node pairs and network control. There are N(N-1)/2 possible links between N nodes. Each antenna beam at each node is positioned by the user with an arrow on the graphical screen display showing node locations and beam positions. Signal levels for links are computed on the basis of actual gains along the link. The jammer will jam the link via receiver and jammer antenna gain levels in those directions.

The received signal power, $P_r$ (dBm) is computed from the transmitters for each of the transmitter/receiver separation distances. The minimum detectable signal $S_{min}$ (dBm) is also computed.

The ratio $P_r/S_{min}$ should be greater than or equal to the required S/N (also supplied by the user in the receiver equipment data file). This check is performed for each transmitter/receiver link. If this ratio is not greater than the required signal-to-noise ratio, then a link between these two nodes is not possible, even without a jammer present.

The received jammer power level $P_{jr}$ that will disrupt communications for each transmitter/receiver link separation is computed using the method described in Section 2.3.5. This

9

is the minimum received jammer power level that causes a successful jamming condition.  These computations are repeated for each position of the jammer if the jammer is not stationary.  The path of motion will need to be specified in either latitude and longitude or azimuth and range.

The outputs for the jammer versus network will be in both tabular and graphical form.  Figure 4 is a graphical output for the jammer versus network scenario type with three nodes attempting to communicate in the presence of jamming.  If the jammer power level at a receiver is within ±3 dB of that necessary to disrupt communications, then the communication quality is considered marginal for that transmitter/receiver pair.  The lines between the nodes are an indication of link quality at the receiver.  Figure 4 indicates that nodes 2 and 3 have a good link in both directions. The link from node 1 to node 2 is marginal, and there is no link from node 2 to node 1.  There is a good link from node 1 to 3, but there is no link from node 3 to 1.  The jammer versus network scenario can evaluate the network performance with or without the jammer present. The user can steer the jammer beam in order to more effectively jam the receiver. The jammer pattern is based on true North and not usually aimed effectively at all of the receivers in the network at once. The angles indicating receiver locations from the jammer are listed on the display screen. The user can enter the angle of the jammer main beam based on true North.  This gives the user the opportunity to optimize jammer beam direction for multiple receivers.  Each time the user runs the scenario, the same questions will be asked after a list of positions is presented on the screen.
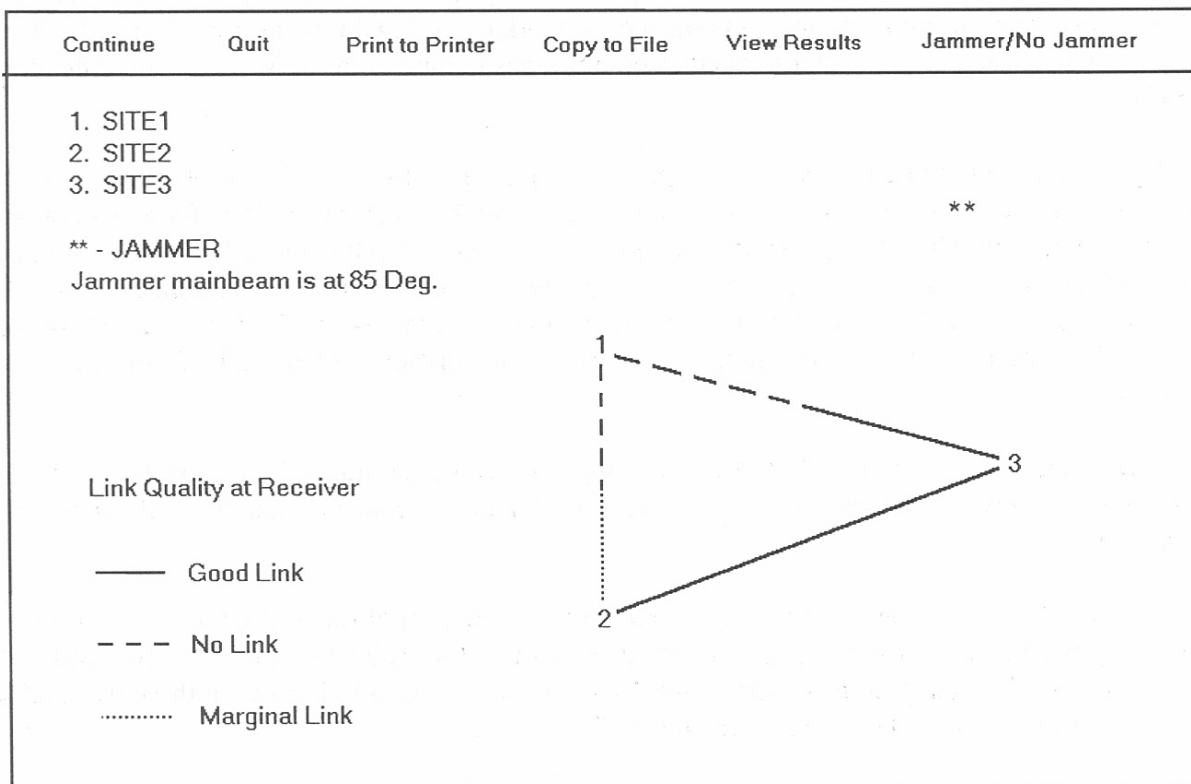


Figure 4. Graphical output display of jammer versus network computation.

The user will be asked to position the jammer beam each time. The user will be able to position the transmitter and receiver beams at each node in the network to provide protection from the jammer and optimize node-to-node communication.


## 2.3 Analysis Models for the Jamming and Jammer Versus Network Scenarios

The computation models described in this section are for the jamming scenario type analyses (jammer footprint, isopower contours, received signal power, received jammer power analyses), and jammer versus network scenario type analyses. The two analyses both share many common models. Those models shared by both the jamming and jammer versus network scenarios will be described together in this section.


### 2.3.1 Antenna Models

The antenna model in the sky-wave model accounts for the variation in antenna pattern gain as a function of elevation and azimuth angle. The antenna model is interactive with the sky-wave computations. The antenna files in the sky-wave model contain the gains for all elevation angles at any of the azimuth angles selected. The appropriate gain is selected by the sky-wave model. The terminated sloping-V, inverted-L, vertical monopole, and the vertical log periodic antennas are the primary high frequency (HF) antennas contained in this model.

The received power from the ground wave and the sky wave are computed separately. These two received powers are combined together to obtain the total received power. Different antenna gains, propagation models, and antenna patterns are used for the HF ground-wave and sky-wave computations. Ground-wave pattern models were generated for these HF antennas and are used by the ground-wave propagation model. The ground-wave antenna patterns are only directional in azimuth in the antenna files. The ground-wave model applies a height-gain function to the antenna pattern gain to provide a modification for elevation angle [4]. The bearing to the receiver and the related offset of the antenna pattern is also computed in a similar manner as the antenna patterns contained in the sky-wave model.

The HF ground-wave patterns are also different from the antenna patterns used with the propagation model for frequencies greater than 30 MHz. Antenna patterns used with this propagation model are fixed one-dimensional arrays with gains for azimuth angles only. The antennas for frequencies greater than 30 MHz include: vertical monopole, dipole, yagi, log periodic, and discone antennas.

The correct antenna gains used in the computation are determined by the bearing to the receiver and the amount of antenna beam offset. The bearing of antenna beams for receivers, transmitters, and jammers is not specified in the data file descriptions for ground stations, aircraft platforms, satellite platforms, or jammers. They are specified by the user by clicking on the platform

location on the screen.  A dial allows the user to steer the beam around 360 degrees.  The beam directions can be specified by the user during the analysis, so that communication effectiveness can be maximized and the effects of a jammer minimized.  This option does not currently exist for the four microwave computational procedures where the antenna beams are pointed at the receivers or transmitters for optimum communication.

All of the antennas discussed above were modeled in order to generate the antenna pattern files for JEM.  In particular, the HF antennas were modeled to create an antenna file to be used by the sky-wave model, the Ionospheric Communications Analysis and Prediction Program (IONCAP) [5].  Accurate modeling was necessary to determine the elevation pattern gain variability for prediction of the actual gain to be used in launching the sky wave at the appropriate take-off angles.  The antenna files with this elevation gain versus angle behavior must be made available to IONCAP by JEM at each degree between zero degrees elevation (grazing incidence) and 90 degrees (zenith).  The antenna gain must also be described at all frequencies in the HF band.  The IONCAP propagation prediction model searches the antenna file for the gains that it needs at different elevation angles, azimuth angles, and frequencies.

IONCAP processes antenna data files that are in a binary format.  This speeds up IONCAP program execution.  An extensive amount of analysis effort was needed to determine antenna pattern behavior with actual gains for each of the antennas.  The data was assembled into the specific antenna file format required by IONCAP and then converted to a binary data file.

The performance of an HF antenna near or on the surface of the Earth is very dependent on the interaction with the lossy Earth.  Currently available techniques using computer algorithms are time-consuming and require conversion or normalization for use in system computations.  The gain of an HF antenna is a function of antenna geometry, materials used to build the antenna, ground conductivity, ground dielectric constant, frequency, elevation angle, and azimuth angle.  The gain required for systems performance analysis is usually referenced to an isotropic radiator in free space or some other reference antenna.  Conventional methods could not be used in this model due to the close proximity of the antennas to a lossy Earth.  The end result of the analysis performed equates the gains referenced to an isotropic radiator in free space.

The antenna analysis was performed assuming that the antenna is not in immediate proximity to other antennas or structures at each site.  It was not possible to model the mutual coupling effects of other antennas and structures for all the possible sites under consideration.  It is assumed that good engineering judgment was used in locating the antennas at all sites so that the major contribution to the performance of the antenna is a result of the antenna design and the lossy Earth on which it was installed.

There are several methods for modeling antennas that are close to a lossy Earth.  Some of these are not valid for an antenna located on the surface.  They require that the antenna be 0.2 wavelengths above the surface. The antenna modeling algorithms that are valid only for antennas greater than 0.2 wavelengths above the Earth should not be used to model antennas in close

proximity to the Earth. The model used for this analysis makes use of extensive method-of-moments calculations and is implemented in a computer program called the Numerical Electromagnetics Code, Version 3 (NEC-3) [6,7]. This model is valid for antennas above the Earth, at the surface of the Earth, and buried beneath the surface of the Earth.

The NEC program uses a computation mode that implements a Sommerfeld integral computation to determine electromagnetic fields for antenna structures that are buried or penetrate the ground-air interface. Examples of these types of antennas include monopoles with ground screens and antennas with ground stakes. This computation technique includes the reflected field below the interface, the field transmitted across the interface, and the fields above the ground-air interface. The algorithms used are also valid for antennas at any distance above or below the interface and at the ground-air interface. The NEC-3 model can also model near fields of the antenna very close to the antenna structure. The far-field and gain computation techniques are also contained in the code. These capabilities are not available in other method-of-moments implementations.

The method-of-moments modeling technique used by NEC-3 requires that the antenna radiating elements be reduced to segments that are a tenth of a wavelength long or less in order to accurately model the antenna structure. For large antenna structures with many elements, this requires many segments to completely describe the model. The algorithm could take as long as one hour to run the patterns and gain of the HF log periodic antenna. This is the reason all of the antenna models at all frequencies are precomputed using NEC-3. The resulting files are reformatted for use in JEM and IONCAP as look-up tables for fast access. The antennas were modeled for all ground constants, and frequencies and files were created for each antenna.


## 2.3.2 Sky-wave and Ground-wave Propagation Models

JEM can perform calculations for receiver distances up to 3000 km. Both the sky-wave and the ground-wave calculations are combined to result in the total signal power for frequencies less than or equal to 30 MHz. The distance increments for each of these calculations have been selected to provide enough data for interpolation, but also to minimize total computation time.

A subroutine computes the latitude and longitude of the points at these distances from the source (transmitter or jammer) to provide IONCAP with a latitude and longitude at the endpoints. A facility has also been added to allow the user to enter range and angle locations with respect to a network control or other station. Bearing and distance or latitude and longitude can be used interchangeably for all analyses.

**The Ionospheric Communications Analysis and Prediction Model**

The sky-wave prediction model is IONCAP. HF communication depends upon the ability of the ionosphere to return the radio signals back to Earth. The ionization of the atmosphere determines the amount of signal that is reflected back to Earth. Prediction of ionization levels in the various

regions of the ionosphere is, therefore, essential to any prediction of HF sky-wave circuit performance. The maximum frequency returned from the ionosphere usually establishes the upper limit of the useful HF range. The degree of ionization in the various regions is useful in estimating probable modes. The transmission loss for these modes is combined with the antenna performance and transmitter power available at the desired times and seasons for any location [5]. The expected sky-wave signal may be compared with the expected radio noise environment to predict the likelihood of the circuit operating satisfactorily. The sky-wave signal prediction in JEM predicts the actual signal level for the analysis frequency for a specific time of day, season, and sunspot number. Additional information on the IONCAP prediction program can be found in [5]; additional information on ionospheric radio wave propagation can be found in [8].

IONCAP requires a number of input parameters in order to perform its computations. The locations of the transmitter and receiver sites must be stated in latitude and longitude. These are supplied from the scenario descriptions in JEM. The transmitter input power is also required and obtained by JEM from the transmitter equipment file. The man-made noise level in a 1-Hz bandwidth that IONCAP uses in its calculations is provided as input from the user as the program is run. This is combined with the atmospheric and galactic noise inside IONCAP using the Spaulding noise model [9] to obtain the total noise level at the receiver. This noise model requires that latitude and longitude of the receiver be specified to determine a noise value. The noise level is also a function of the radio frequency and the receiver bandwidth. The month, time, and sunspot number are also provided by the user when the program is run.

IONCAP calculates a myriad of HF sky-wave propagation parameters to perform a complete system analysis. Typical parameters calculated include: median values of Maximum Useable Frequency (MUF), Frequency of Optimum Transmission (FOT), Lowest Usable Frequency (LUF), field strength, reliability, antenna gain, noise power, system loss, received signal power, received electric field strength, and signal-to-noise ratio. IONCAP contains the latest International Telecommunications Union-Radio (ITU-R)-approved atmospheric noise coefficients, improved man-made noise calculations, and more realistic specifications/predictions for the global variations of the F-region critical frequencies.

Most variations of HF system performance are directly related to changes in the ionosphere, which in turn are affected in a complex manner by solar activity, seasonal and diurnal variations, and latitude and longitude. IONCAP uses table look-up techniques quite extensively to reduce computer run time [5]. IONCAP has seven subroutines, two of which are associated with input and output functions. These input and output subroutines interface with JEM. The remaining five categories of subroutines perform the calculations for ionospheric propagation analysis: path geometry, antenna gain, ionospheric parameter, maximum usable frequency, and system performance computations.

The path geometry subroutines determine the HF circuit geometry, select the areas where the ionosphere is, and evaluate the magnetic field in these sample areas. The antenna subroutines calculate the antenna gains and patterns and determine the actual gains at different azimuth and

take-off angles for different frequencies and ground parameters. The ionospheric subroutines evaluate the ionospheric parameters using an explicit electron density profile represented by the E and F2 layers which are assumed to be parabolic. The profile consists of a D-E region starting at 70 km, an F2 region, an F1 ledge, and an E-F valley [5]. An empirical modification to the secant law is also included in this program. The maximum usable frequency subroutine determines the junction frequency directly from an electron density profile derived from monthly median parameters of the ionosphere [5]. The MUFs of the E, F1, and F2 layer are all considered. The system performance subroutines evaluate circuit performance parameters, but JEM primarily uses the received signal power, electric field strength, and noise level. The method for computing noise is described by Spaulding [9, 10].

The ionosphere has several layers (D, E, F), but the most dominant contributor to HF propagation is the F layer, because of its total population of electrons or electron content. The F layer does not always have a one-to-one correspondence with radio-wave propagation effects. The lower layers (D,E) may have a major impact on HF operation, because of geometrical factors or collision processes. In some instances the impact of these lower layers may be the controlling factor in propagation. The normal D layer is the lowest altitude layer and is characterized by radiowave absorption causing it to act as a power-robbing attenuator. The D layer has this characteristic in the daytime when the sun's photo ionization flux is greatest. On some occasions the sporadic E layer ionization may cause the E layer to serve as the primary reflecting layer as it blankets the upper ionospheric layers [11].

**The HF Ground-wave Model**

The ground-wave model within the JEM computes ground-wave propagation loss over smooth homogeneous Earth. This model was described by Berry [12] and is also described in more detail in [13,14]. The ground wave includes the direct line-of-sight space wave, the ground-reflected wave, and the surface wave that diffracts around the curved Earth.

The formulas used in the smooth-Earth model are adapted from Abramowitz and Stegun [15], Wait [16], Fock [17], King [18], and Hill and Wait [19]. The following six computation techniques are used: flat-Earth attenuation function, flat-Earth attenuation function with curvature correction [19], Hill and Wait's series for small Q [19], the residue series calculation [16, 17], geometric optics [13], and numerical integration of the full-wave theory [13]. The flat-Earth attenuation function with curvature correction and Hill and Wait's series for small Q were added in 1984 by L.A. Berry [20].

Antenna heights, path lengths, Earth geometries, ground constants, and frequency are used by the program to automatically select the appropriate computation technique. The losses calculated by the smooth-Earth method are in agreement with [21], where Norton's approximations are valid, and the CCIR curves [22]. The smooth-Earth method is mathematically and numerically accurate for the ground-wave predictions for frequencies from 10 kHz to 100 MHz [12]. Above 30 MHz, the irregularities of the atmosphere make statistical methods more appropriate. Irregularities in

the terrain have more of an effect at higher frequencies, so an irregular terrain model is more appropriate when terrain irregularities become appreciable in size with respect to a wavelength.

The smooth-Earth method calculates field strength and converts this to propagation loss. The computation technique depends on the relative geometry of the transmitter and receiver locations, the ground constants, and the radio frequency. The radio wave propagates as a surface wave when both the transmitter and receiver are near the Earth in wavelengths. If, in addition, the path lengths are short such that the Earth can be assumed to be flat, then the flat-Earth attenuation function [16] is valid. The equations are given in [14].

When the transmitter and receiver are high enough that an observer at the receiver or transmitter is well above the radio horizon when viewed from the other, the field strength computation involves the use of geometrical optics. The formulas are given in [14].

When the receiving antenna is near the radio horizon of the transmitting antenna, the field depends on diffraction effects in addition to the direct wave, and in this case the computation technique is performed by numerical integration of the full-wave theory integral [14].

For long path lengths, the Earth cannot be considered flat. If, in addition, the geometry is such that a straight line connecting the transmitter and receiver antennas intersects the curved Earth, then the full-wave theory integral must be evaluated using the residue series [16,17].

For cases where the antennas are close to the Earth but the path lengths are long, the field-strength computation is performed using either a flat-Earth attenuation function with a small-Earth curvature expansion or a power series expansion. These two techniques are for the purpose of reducing the use of the numerical integration of the full-wave theory integral, since it is very time-consuming. These two techniques bridge the gap for loss computation between the case where the Earth is flat (flat-Earth attenuation function) and that where the receiving antenna is near the radio horizon of the transmitting antenna. The computation technique is selected depending on the magnitude of a factor q [19]. The factor q is:

$$q = -i\Delta(Ka/2)^{1/3} \ ,$$

where

$K = 2\pi/\lambda,$

$\lambda$ = wavelength of radio wave (meters),

$a$ = radius of the Earth (meters), and

$\Delta$ = normalized surface impedance of the ground below the antenna in question.

If the polarization is vertical, then $\Delta$ is:

$$\Delta = \frac{\sqrt{\in_{gc} - 1}}{\in_{gc}}$$

if the polarization is horizontal, then $\Delta$ is:

$$\Delta = \sqrt{\in_{gc} - 1}$$

$$\in_{gc} = \in_g + \frac{\sigma_g}{i\omega \in_o}$$

$$i = \sqrt{-1} \quad ,$$

where

$\in_{gc}$ = complex dielectric constant of ground,

$\in_g$ = the relative dielectric constant of ground,

$\sigma_g$ = conductivity of the ground in siemens/meter,

$\in_o$ = permittivity of free space 8.85 x $10^{-12}$ farads/meter,

$\omega = 2\pi f$, and

$f$ = the operating frequency in Hertz.

The surface impedance is a function of the ground constants of the Earth's surface. If the magnitude of q is small (less than 0.1), then a power series expansion is used for the attenuation function [23,24,25]. The attenuation function is the ratio of the electric field from a short dipole over the lossy Earth's surface to that field from the same short dipole located on a flat perfectly conducting surface.

If the magnitude of q is large (greater than 0.1), then a small-curvature expansion is more appropriate for the attenuation function [20,23]. The implementation of these two techniques reduces the need for the numerical integration technique and reduces computation time considerably.

The smooth-Earth model is valid for all combinations of antenna heights, frequency, and dielectric constants by virtue of the six computation techniques contained within its structure. It should only be used for distances considered useful for ground-wave propagation at each frequency, since the sky wave would become significant from that distance to points beyond. This distance is roughly 300 km at low frequencies (less than 0.5 MHz) and depends on frequency. The actual effect on distance must be determined for each frequency. The distance decreases with increasing frequency. The ground-wave model is valid for path lengths ranging from 1 to 10,000 km, where the actual distance is dependent on frequency [12].

**The Irregular Terrain Model**

The ITS Irregular Terrain Model (ITM) is sometimes called the Longley-Rice Model [26,27]. It is valid from 20 MHz to 20 GHz for a wide variety of distances and antenna heights. It calculates received power level but does not analyze channel characterization or waveform modeling. The model includes not only the average level of received power, but a statistical description of the received signal variability. The received signal level will actually vary in time due to changing atmospheric conditions that cause refraction effects. The signal will also change in space due to a change in terrain along the propagation path.

The ITM is both an area prediction model and a point-to-point model. The area model refers to a link or broadcast station for which much of the specific information is either nonexistent or unavailable. This would include a mobile commercial link, a military tactical unit, or a radio station broadcasting to a large number of receivers. The terrain along the path is difficult to characterize specifically. The terrain irregularity parameter is only estimated from a general knowledge of the site location. The JEM model uses the ITM area prediction mode, because there are currently no terrain databases within the JEM libraries. The area mode of ITM is well-suited in JEM. A point-to-point model refers to a specific communications link where detailed information about the link will be available including the actual terrain in between the endpoints. This would include fixed or semipermanent communication links.

JEM provides several important system and environment parameters to ITM so that it may calculate the received signal level. These parameters are supplied via the scenario descriptions. The system parameters include: frequency, distance, antenna heights, and antenna polarization. The frequency is the carrier frequency of the transmitted signal. The distance is provided by the JEM algorithms and is computed from the locations listed in the scenario description between the jammer, transmitter, and receiver. The antenna heights are the center of radiation above ground level. Antenna heights can be difficult to obtain and are described further in [26]. The antenna polarization is that of both antennas and is assumed to match for both the source and the receiver.

The environmental parameters are independent of the system and describe the statistics of the environment in which the system operates. The environmental parameters include: the terrain irregularity parameter, two ground constants (relative permittivity and conductivity), surface refractivity, and climate. The terrain irregularity parameter is a single value that describes the size of the terrain roughness for each path that characterizes the random terrain. The terrain irregularity parameter ranges from zero to 500 for a terrain ranging from a flat surface to an area with rugged mountains, respectively. The ground constants available include those for poor, average, and good ground, in addition to sea water. The surface refractivity ($N_s$) and the climate characterize the atmosphere and its variability with time. The condition of the atmosphere due to climate and weather determine the surface refractivity. How this refractivity changes with height is termed the refractive index gradient. This refractive index gradient determines how much a radio ray is refracted in the atmosphere. The "effective" radius of the Earth is a function of $N_s$. An extensive description of the ITM parameters can be found in [26].

ITM determines the position of the radio horizons from propagation equations, geometry, and the terrain irregularity parameter. The model then determines a reference attenuation as a function of distance and the radio horizon. There are three regions of markedly different reference attenuation behavior: line-of-sight, diffraction, and forward scatter. The calculations are performed using theoretical techniques of reflection from rough ground, refraction through a standard atmosphere, diffraction around the Earth and knife edges, and tropospheric scatter. These theoretical techniques are combined with empirical relations that were determined by curve-fitting to measured data. The theoretical techniques are described in detail in [28] and the original Longley-Rice report [27]. The measured data is based on that taken as part of a large measurement program [29]. The prediction technique of ITM is based on measured data and theoretical techniques obeying physical laws of radio wave propagation.

The low frequency limit for ITM was set at 20 MHz, since ionospheric propagation is likely to occur below this frequency. JEM runs ITM only above 30 MHz and uses a combination of ground-wave and sky-wave propagation models for 2- to 30-MHz performance predictions.

The upper frequency limit for ITM was set at 20 GHz, because of atmospheric absorption due to the water-vapor line at 22 GHz. These phenomena are not taken into account, but may be ignored below 10 GHz without much effect on the total attenuation except on very long paths. The attenuation due to rainfall is also ignored in ITM. Rainfall attenuation becomes important above about 6 GHz, but is measurable only during very heavy rainstorms which take place only about 1% of the time [26]. These effects of clear-air absorption attenuation and rain attenuation are taken into account in the original four scenarios and may be used to determine the significance of the magnitude of these effects.

ITM can cause problems for prediction of line-of-sight point-to-point microwave links that have adequate Fresnel zone clearance [26]. Along such a link the propagation loss is just the free-space loss over the distance. ITM does not assume an adequate Fresnel clearance except on very short paths, so by its very nature will add attenuation to the free-space or median reference attenuation.

ITM incorporates statistical calculations to allow for time and location variability. The model only accounts for long-term time variations. It does not account for the rapid scintillations of signal level associated with short-term variability or "rapid fading" indicating how the signal varies over periods less than an hour. These short-term variations are accounted for by fade margins, diversity, robust modulation techniques or a combination of these.

Three types of statistical measures are used to characterize long-term variability in the ITM model within JEM: the time availability, location variability, and situation variability. The time availability is the fraction of time during which an adequate signal is available. The location variability is the fraction of the local area in the immediate vicinity of the receiver that will receive an adequate signal level. The value of signal level predicted after considering time availability is for an average location, which is the average of many different locations in the immediate vicinity of the receiver location. The combination of time availability and location variability results in a prediction of the fraction of the time that a certain percentage of the locations will receive a certain signal level. The situation variability factors in the variation in the propagation loss measurements and indicates the percentage of the measurements that have signal levels greater than or equal to the predicted signal. All of these variabilities have been set to 50% to minimize the variations and represent a signal level that is available 50% of the time, in 50% of the immediate locations about the receiver. The model's predicted transmission loss is greater than or equal 50% of the measured losses on which the model is based. A complete and detailed account of the statistical description of ITM is contained in [26].


### 2.3.3 Model for Computing Received Signal Power From a Transmitter

The method used to compute signal power received from either a transmitter or jammer depends on the frequency. If f is less than or equal to 30 MHz, both a ground-wave signal power level (using GW84) and a sky-wave signal power level (using IONCAP) are computed separately and then combined to determine the total signal power. If f is greater than 30 MHz, only a ground-wave signal power (using ITM) is computed.

For HF computations (f less than or equal to 30 MHz), GW84 is used to compute the propagation loss $L_p$(dB) for the ground wave. $L_p$(dB) is a function of frequency, antenna height, and distance between the transmitter or jammer. It is also a function of the ground conductivity and permittivity between the source and the receiver. Using this loss and the system parameters for the transmitter/receiver link the received signal power due to the ground wave is computed for each transmitter/receiver separation.

The ground-wave signal power from the transmitter is:

$$P_g = P_t + G_t + G_r - L_p \quad ,$$

where

$P_t$ = the transmitter power in dBm,

$G_t$ = the transmitter antenna gain at the appropriate azimuth angle in dB, and

$G_r$ = the receiver antenna gain at the appropriate azimuth angle in dB.

The following equations are used to combine the ground-wave and sky-wave signal power from a transmitter:

The sky-wave signal power from IONCAP is $S_s$ in dBW and must be converted to dBm. $S_s$ (dBm) = $S_s$ (dBW) + 30. It is then added to the ground-wave signal power $P_g$.

$P_r$ (dBm) is the total jammer power into the receiver from combining $P_g$ (dBm) and $P_s$ (dBm) by addition of their actual power in mW. The power must be converted from dBm to mW before the addition is performed, and the result is then converted back to dBm:

$$P_g \text{ (dBm)} = 10 \log P_g \text{ (mW)}$$

$$P_s \text{ (dBm)} = 10 \log P_s \text{ (mW)}$$

$$P_r \text{ (mW)} = P_g \text{ (mW)} + P_s \text{ (mW)}$$

$$P_r \text{ (dBm)} = 10 \log P_r \text{ (mW)} \ .$$

$P_r$ is the total received power from the transmitter from combining $P_g$ and $S_s$.

The same equations are used to combine the ground-wave and sky-wave signal power from a jammer. The transmitter power is replaced by the jammer power $P_j$, and the transmitter antenna gain is replaced by the jammer antenna gain $G_j$.

**2.3.4 Receiver Sensitivity Computation Model**

The computation method for receiver sensitivity $S_{min}$ (dBm) is dependent on the frequency. For HF frequencies (f less than or equal to 30 MHz), the receiver sensitivity must be calculated from receiver parameters and the external noise level from the IONCAP noise file. The equation for this is:

$$S_{min} = 60 + 10 \log BW + NF + NI \quad ,$$

where

Smin = the receiver sensitivity or minimum detectable signal power in dBm,

BW = the receiver bandwidth in Hz,

NF = receiver noise figure in dB, and

NI = total noise power from IONCAP output file in dBW.

For frequencies greater than 30 MHz, the receiver sensitivity must be calculated from receiver parameters only and not the external noise level from the IONCAP noise file. The equation for this is:

$$S_{min} = \text{-174 dBm/Hz} + 10 \log BW + NF \quad .$$

## 2.3.5 Jammer Power Level That Will Disrupt Communications

The jammer footprint and the jammer versus network use a simple relationship to compute the received jammer level $P_{jr}$ (dBm) necessary to disrupt communications for each transmitter/receiver separation or network link, respectively:

$$P_{jr} = J/S + P_r \quad ,$$

where

J/S = the maximum jammer signal to received signal ratio in dB with which the receiver can still operate in the presence of jamming, and

$P_r$ = the received power from the desired transmitter in dBm.

J/S is obtained from the receiver equipment data file and can be changed by the user.

## 3. THE MICROWAVE COMMUNICATION SCENARIOS

The propagation models in the four microwave communication scenario types differ significantly from those models used in the jamming and jammer versus network scenario types. They cover a higher frequency range and must therefore include clear-air absorption losses and losses due to rain attenuation. This section briefly describes each of the analysis models in the four microwave communication scenario types (ground-to-satellite, ground-to-aircraft, aircraft-to-satellite, and

ground-to-ground). All of the analysis models were first implemented in computer code in the ETSEM computer program and are described in complete detail in [1].


### 3.1 Models for Earth-to-satellite Scenario

The Earth-to-satellite scenario type contains two analysis models. One calculates the cumulative distribution of rain attenuation over the months specified by the user. The other calculates the cumulative distribution of clear-air attenuation over the months specified by the user. Both of these analyses compute these losses over the path between the ground station and a point on the satellite orbit file (selected by the user). The satellite orbit file contains the positions of the satellite in its orbit path. The positions in this file are specified by latitude, longitude and altitude. The calculations can be performed for different climates. The climate is set in the scenario by either manually filling the array with rain rate, humidity, etc. by month, or by filling from the database. When filling from the database, the user is asked to indicate latitude and longitude.

The rain attenuation model only calculates the rain attenuation above free-space loss. The calculation of received signal level requires adding the free space loss to this rain attenuation; the free-space loss is not computed in this analysis. The output of this model contains the percentage of time that the rain attenuation losses are exceeded. The model calculates the loss exceeded for a certain percentage of the time for the user selected time period and geographic location. The time period is designated by months. For example, if the loss exceeds 11.4 dB for .05% of the time at a specific location for the month of May, then the loss due to rain attenuation is less than 11.4 dB for 99.95% of the time. For the month of May .05% of the time is 22.32 minutes.

The clear-air attenuation model only calculates the clear-air attenuation above free-space loss. The calculation of received signal requires adding the free-space attenuation to this clear-air attenuation loss; the free-space loss is not computed for this analysis. This model determines the percentage of time that the clear-air attenuation losses are exceeded. The cumulative distribution of atmospheric water vapor pressure is used to model the cumulative distribution of clear-air attenuation. The water vapor pressure for a specific percentage of time is determined and then that value of water vapor pressure is used to calculate the clear-air attenuation [30]. The clear-air attenuation is calculated using average ground conditions based on data from 40 cities in the United States. A least square progression between the data points for the 40 cities is performed so that the cumulative distribution can be obtained.

The point rain rate for the cumulative distribution of rain attenuation was modeled using Crane's algorithm [31] for a point-to-path conversion between the point rain rate and the rain attenuation. This model is used by the CCIR and has been shown to be one of the better models for rain attenuation [32]. The actual implementation of Crane's model is completely described in [1]. A modification of the Rice-Holmberg algorithm [33] was used to model the point rain rate distribution. The Rice-Holmberg model determines the rain rate distribution in terms of commonly recorded climatological parameters. It calculates the amount of time that the point rain

rate in mm/hr is exceeded as a function of the rain rate, the total precipitation in mm, and a thunderstorm ratio (fraction of rainfall from convective storms). It is desired to have monthly predictions of performance for short-term tactical deployments, but the statistics for thunderstorm ratio given in the Rice-Holmberg model are a function of yearly statistics. An alternate formulation for the thunderstorm ratio was developed in [1] that could use available monthly statistics instead of yearly statistics.

The specific attenuation A (dB/m) through rain has been shown analytically and experimentally to be related to the rain rate RR (mm/hr) and the a and b coefficients from the work of Olsen, Rodgers, and Hodge [34]. The equation relating these coefficients and rain rate to specific attenuation is:

$$A = a(RR)^b$$

However, Allen [1] has found that the a and b coefficents of Joss et al. [35] have a better fit to measured data. The coefficients of Joss were used in this model.

Modifications to the rain attenuation model were made to account for the slant range between the Earth and the satellite. Additions to the model were also made to account for atmospheric layers below freezing. For such layers below freezing there can be no rain and hence no rain attenuation. These modifications are described in [31].

The Earth-to-satellite analysis for rain attenuation requires data describing the climate and the satellite orbit flight path. A point on the satellite flight path is described by the latitude, longitude, and altitude of a satellite. This analysis also requires rain attenuation coefficients to compute rain attenuation and isotherm profiles to calculate the zero degree isotherm height.

### 3.2 Models for the Ground-to-air Scenario

The ground-to-air scenario type contains four analysis models. The first model calculates the attenuation and received signal level for a loop of frequencies over a single path between the ground station and a single user-selected point on the aircraft flight path. The second model calculates the attenuation and received signal at a single frequency for a loop of multiple positions over the path between the ground station and the points on the aircraft flight path. The attenuation and received signal level calculated include the free-space loss, the median long-term clear-air attenuation (due to oxygen and water vapor absorption), and the diffraction losses for the user-specified atmospheric conditions according to the methods contained in [36]. Losses due to rain attenuation are not included in either of these two models.

The third and fourth models calculate the cumulative distribution of rain attenuation and clear-air attenuation, respectively, over the months specified by the user. Both of these analyses compute these losses over the path between the ground station and a user-selected point on the aircraft

flight path. Both of these models calculate the additional attenuation due to clear-air absorption or rain above free-space loss. The calculation of received signal level includes the addition of free-space loss to the rain attenuation or clear-air attenuation. The output of each of these two models contains the percentage of time that the rain or clear-air attenuation losses are exceeded for the user-selected time period and geographic location. The calculations are geographic location sensitive. The time period is designated by months. The rain rate is selected by the user for the rain attenuation computation.

The fourth analysis model contains the cumulative distribution of clear-air attenuation and only calculates the clear-air attenuation above free-space loss due to oxygen and water vapor absorption using the water vapor and oxygen line interpolations described in [36,37]. This calculation includes the dispersive and nondispersive terms for dry air, water vapor, suspended water droplets, and rain. The specific attenuation at the desired heights is calculated and multiplied by the appropriate path lengths to obtain the attenuation along the path. The clear-air attenuation is modeled as the sum of a dry air term and a water vapor term according to a procedure described in [1]. A normally distributed probability function was used and is based on a technique by Bean and Cahoon [38] for absolute humidity. Bean and Cahoon modeled the cumulative distribution of absolute humidity in $g/m^3$ by giving the humidity exceeded 90, 95, and 99% of the month in terms of the mean absolute humidity for the month.

The first and second ground-to-air analyses require the atmospheric data file. The third and fourth ground-to-aircraft analyses require the climate data file, horizon data file, and an aircraft flight path data file. The third analysis that computes the cumulative distribution of rain attenuation requires a file with the rain attenuation coefficients. All four of the analyses require the horizon data file and an aircraft flight path data file.

The atmospheric profile data is in an ASCII file that describes three parameters of the atmospheric layers. The first parameter is the height of the atmospheric layer above ground in kilometers. The second parameter is the average temperature of the atmospheric layer in degrees Centigrade. The third parameter is the relative humidity in percent of the layer.

The horizon file contains: the azimuth angle to the horizon in degrees East of true North, distance to the horizon point in kilometers, and the elevation in meters above mean sea level at the horizon point. There can be as many as 360 sets of data for 1 to 360 degrees in the horizon data file. The aircraft flight path data file contains the points that describe the aircraft flight path in latitude and longitude. The elevation in meters above mean sea level is also specified. The climate file contains the mean number of days of precipitation greater than 0.25 mm, the mean number of days of thunderstorms, the mean precipitation amounts in mm, the mean temperature in degrees Celsius, and the mean relative humidity for each month of the year. In addition, an oxygen and water vapor line coefficients database is required.

### 3.3 Models for the Aircraft-to-satellite Scenario

The aircraft-to-satellite scenario contains three analysis models. The first analysis calculates the attenuation and received signal level for a single frequency over a path between a set of points on a user-selected flight path of the aircraft and a fixed point on the satellite orbit. The second analysis calculates the attenuation and received signal level for a range of user-selected frequencies over a path between a fixed point on the aircraft path and a fixed point on the satellite orbit. The third analysis calculates the attenuation and received signal level for a single frequency over paths between the points on an aircraft flight path and a satellite orbit path. The propagation losses that are considered in all three analyses are limited to free-space, clear-air attenuation, and rain attenuation. The rain rate is selected by the user.

This analysis uses the same external data files that are used in the analyses of clear-air and rain attenuation. This analysis uses Liebe's atmospheric millimeter wave model [36] to determine clear-air and rain attenuation except that the user can choose a nonzero rain rate. The atmospheric profile data files are required for all three analyses in the aircraft-to satellite scenario type.

### 3.4 Models for the Terrestrial Scenario

The terrestrial scenario contains six analyses for performing different computations between two ground stations over irregular terrain. The first analysis calculates the cumulative distribution of rain attenuation for the terrestrial path over a range of months selected by the user. The attenuation calculation considers only the rain attenuation. The user must add the free-space loss to the rain attenuation. The physical models for the cumulative distribution of rain attenuation of the first analysis are identical to those used in the Earth-to-satellite analysis of Section 3.1. The databases used in this analysis are also the same.

The second analysis calculates the cumulative distribution of multipath attenuation for the worst month. The only loss considered in this computation is the multipath loss over free-space loss. The user must add the free-space loss to the multipath loss. The physical model for the cumulative distribution of multipath attenuation is the multipath fading model developed by Crombie [39]; the implementation of this model is completely described in [1]. The model gives the percent of the worst month that a given multipath attenuation is exceeded. The model depends on the beamwidths of the receiver and transmitter antennas, the average height of the center of the path, the frequency, and the path length; the model was developed for frequencies greater than 10 GHz. This analysis requires a terrain data file; this file contains the terrain heights at different distances along the path between the ground stations and the heights of obstacles at each of these points to describe the obstacles along the path. This analysis also requires the climate data file.

The third analysis plots the terrain path and the ray path and the Fresnel clearance envelope (specified by the user). This analysis also calculates the antenna heights in order to ensure a Fresnel clearance over this path. The analysis uses a terrain profile created by the user, the

ground station data, and the scenario data to plot the terrain profile and ray path. The geometry is based on the theory presented in Section 4.2.15 of [40]. The Fresnel zone clearance for any obstacles along the path is calculated using the equations from Section 4.2.18 of [40]. The equations used for these calculations are described completely in [1]. This program requires the terrain profile data file.

The fourth analysis calculates the cumulative distribution of the clear-air attenuation over the range of months specified by the user for the path between two ground stations. The only propagation loss considered is the clear-air attenuation above free-space loss. The user must add the free-space loss to the clear-air attenuation loss. These calculations use the same algorithms as those for the Earth-to-satellite analysis in Section 3.2. The recent atmospheric millimeter-wave propagation model by Liebe [36] is used for calculating complex refractivity. The specific attenuation is derived from the complex refractivity. The specific attenuation is multiplied by the path length to obtain the atmospheric attenuation along the path. This calculation requires the climate data file.

The fifth analysis can calculate either the median long-term troposcatter loss or the median long-term diffraction loss for terrestrial paths that are not line of sight. The free-space losses are included in this analysis. This analysis requires the terrain profile data file, the climate data file, and two horizon data files.

The sixth analysis determines the link margin for a terrestrial path for each of the twelve months of the year. The propagation loss effects that are considered include: clear-air attenuation, free-space loss, diffraction, and troposcatter. This analysis requires the same four data files as those in the fifth analysis.


## 4. SUMMARY

The Jammer Effectiveness Model is a user-friendly and menu-driven computer program that was developed to analyze the effectiveness of a jammer in jamming a receiver/transmitter pair or a network of receivers and transmitters. It also contains models for evaluating and designing microwave communication systems. This allows a user to simulate a wide variety of propagation effects on a system.

The JEM was created by adding new jamming scenario types to the AMOS program. The result is a very flexible and powerful collection of analysis software that contains a total of six scenario types each performing a different function. A scenario type represents a communication path geometry description (ground-to-ground, ground-to-satellite, ground-to-aircraft, and aircraft-to-satellite), or jamming geometry description (jamming or jammer versus network). For the two jamming geometry scenarios, the model can perform an analysis on a ground-based airborne receiver, transmitter, or jammer platforms. The remaining four scenario types can be used as an

aid in evaluating and designing microwave communication systems. They allow the user to analyze a wide variety of propagation effects on the system.

The JEM is highly structured and modular in design, allowing greater flexibility and expandibility. The JEM includes: a user-created catalog of equipment, ground stations, and aircraft and satellite platforms; the software for creating and maintaining this catalog; a climatological database for much of the world; a library of propagation subroutines; and the analysis software. The analyses include subroutines for use in calculating clear-air attenuation, rain attenuation, multipath attenuation, diffraction, and troposcatter.

The jamming scenarios of the JEM can be used for analysis in the frequency range of 2 MHz to 20 GHz. The 2- to 30-MHz range includes propagation models for both the ground wave and the sky wave. An irregular terrain model for the 20-MHz to 20-GHz frequency range has also been integrated into the JEM. The four microwave communication scenarios have analyses that are valid for the evaluation and design of microwave communication systems operating between 1 and 300 GHz.

## 5. RECOMMENDATIONS

Although the JEM is a complete model that can perform a wide variety of communications and jamming analyses, certain aspects could be updated or improved.

1.    The original four microwave communication scenarios currently run as DOS applications in Windows. They do not run as Windows applications in Windows. Modifying these scenarios to run as Windows applications would allow these scenarios to interact more effectively with the rest of the JEM.

2.    The inclusion of rain and clear-air attenuation into the jamming scenarios is also recommended. This would allow these effects to be included at frequencies above 6 GHz, thus resulting in more accurate modeling in the jamming scenario types.

3.    A more extensive multipath model based on recent research should be incorporated to obtain more accurate predictions of mobile communications in a severe multipath environment. Simulating the effects of multipath in the radio propagation channel is important for both short and long distances. The channel modeling would include the effects of multipath in a more detailed manner than that currently existing in the JEM.

4.    In the current version of the JEM, actual terrain data can be currently used in only the terrestrial scenario of the four microwave analysis scenarios, but

cannot be used in the jamming scenarios. ITM uses a delta h factor to represent terrain roughness, but does not use a terrain data base. This works well for many applications, but determining propagation loss with an actual terrain description would be more accurate. ITM could be run in the point-to-point mode to use terrain files, but a capability to interface the terrain database to ITM within the JEM is required. The low frequency ground-wave model (f less than or equal to 30 MHz) can also be modified to accept terrain files. Software must be developed to interface the terrain files with the propagation models within the JEM.

5. The phenomenon of skip distance for ionospheric propagation is not addressed by the JEM. The models within the JEM can predict the skip phenomenon, but it is not communicated to the user directly. For example, when computing received power from a source, the program will compute the actual received power and show where the signal increases due to the enhancement of the sky wave because of ionospheric propagation. However, if the user is not looking at the appropriate ranges, the skip phenomenon is not apparent. This can also happen with the isopower contour predictions of power density. The user could accidentally stumble on two contours for one power density or see a higher power density further out in range due to the enhancement of the sky wave. An algorithm needs to be developed to search for and identify the presence or possibility of the skip phenomenon.

6. Calculating the area of the jammer footprint in the jamming scenario analysis for each contour generated is another feature that would be useful. The area jammed can be used as a measure of effectiveness for system jamming analyses.

7. The current analysis technique determines how much sky-wave signal power is received at the desired analysis frequency. It is not performed at the optimum frequency for sky-wave propagation. It would be useful to know what frequency or frequencies would be more optimum for ionospheric propagation for a particular link analysis.

8. The jammer versus network analysis predicts the effectiveness of only one jammer in jamming the victim network. It would be useful to determine the effectiveness of multiple jammers against the network.

9. The JEM currently computes received power and received power density in the analyses incorporating the appropriate propagation loss. However, effects of the particular waveform to the signal are not included. This is currently accounted for by the signal-to-noise ratio required for adequate operation. The signal-to-noise ratio is entered by the user into the receiver data file of

equipment database. The user must know this signal-to-noise ratio for the system being analyzed. These waveform effects should be included to more completely characterize the propagation phenomena.

10. The addition of latitude and longitude by city index as an on-line access capability can be included in the equipment database.

11. The current scenarios in the JEM do not provide for the analysis of radar performance in a jamming environment. The addition of a radar jamming scenario to the JEM would provide for the performance analysis of target detection and tracking in a jamming environment.

All of the above suggestions are independent and can be incorporated into the JEM separately. Items 1, 3, 4, 5, 9, and 11 are major efforts and would require extensive work to complete. Item 1 requires that the four microwave scenarios be converted to code appropriate for Windows operation. Each of the analyses of each scenario would also have to be converted. Item 3 involves adding improved multipath models to the JEM. A model that simulates the effects of multipath would involve generating models based on extensive data collected recently by ITS. This modeling, measurement, and simulation effort for Item 3 is also a significant effort. ITS is currently developing multipath models based on recent research in this area. Item 4 would require the software development of code that would interface the terrain files to the propagation models. This work is currently underway at ITS for the low frequency ground-wave model. The skip distance computation technique required in Item 5 needs to be developed. Incorporating waveform effects into the JEM for link analyses would require an extensive analysis effort for those particular waveforms that would be needed for completion of Item 9. The JEM currently analyzes communication system performance in a jamming environment. It is not capable of analyzing radar system performance with or without the jamming environment. Item 11 would add this capability to the JEM and would require adding a new scenario and extensive modification of the propagation models.

Items 2, 6, 7, 8, and 10 can be implemented easily. The inclusion of the rain and clear-air attenuation calculations in the jamming scenarios of Item 2 is relatively easy to implement by integration of the appropriate propagation models from the microwave scenario analyses. These would be even easier if the original four scenarios were operating in Windows. The calculation of the area of the jammer footprint will require development of an algorithm to determine the area of the footprint for Item 7. The sky-wave model in the JEM can be easily be configured to predict optimum sky-wave communication frequencies for a particular link analysis for Item 7. The addition of multiple jammer capability for Item 8 will require generation of more user input and output interfaces to describe the scenarios created by multiple jammers to the JEM and also provide for data output presentation to the user. This is a relatively simple modification for a few jammers. The addition of a latitude and longitude database by city name (Item 10) would be an easy addition to the JEM providing the database exists in a compatible format.

# 6. REFERENCES

[1]  K.C. Allen, "EHF telecommunication system engineering model," NTIA Report 86-192, April 1986. (NTIS Order No. PB 86-214814/AS).

[2]  K.C. Allen, "Software for the analysis of microwave operational scenarios," in *Proc. of the IEEE Commun. Society,* 1990 IEEE Military Communications Conference, Washington, D.C., 1990, pp. 17.5.1-17.5.5.

[3]  J. Geikas and N. DeMinco, "Jammer Effectiveness Model," NTIA Report 95-317, November 1994.

[4]  N. DeMinco, "Ground-wave analysis model for MF broadcast systems," NTIA Report 86-203, September 1986, (NTIS Order No. PB 87-124293/AS).

[5]  L.R. Teters, J.L. Lloyd, G.W. Haydon, and D.L. Lucas, "Estimating the performance of telecommunications systems using the Ionospheric Communications Analysis and Prediction Program User's Manual," NTIA Report 83-127, July 1983, (NTIS Order No. PB 84-111210).

[6]  G.J. Burke and A.J. Poggio, "Numerical Electromagnetics Code (NEC) method of moments, parts I, II, III," Naval Ocean Systems Center Report NOSC TD 116, NEC-l (1977), NEC-2 (1981), NEC-3 (1983).

[7]  G.J. Burke and E.I. Miller, "Modeling antennas near to and penetrating a lossy interface," Lawrence Livermore National Laboratory, UCRL-89838, 1983.

[8]  K. Davies, "Ionospheric radio propagation," NBS Monograph 80, April 1965.

[9]  A.D. Spaulding and F.G. Stewart, "An updated noise model for use in IONCAP," NTIA Report 87-212, January 1987, (NTIS Order No. PB 87-165007/AS).

[10]  A.D. Spaulding and J.S. Washburn, September, "Atmospheric radio noise: worldwide levels and other characteristics," NTIA Report 85-173, September 1985. (NTIS Order No. PB 85-212942).

[11]  J. Goodman, *HF Communications, Science and Technology,* New York, New York: Van Nostrand Reinhold, 1992.

[12]  L.A. Berry, "User's guide to low frequency radio coverage programs," Office of Telecommunications Technical Memorandum 78-247, January 1978.

[13] L.A. Berry and J.E. Herman, "A wave hop propagation program for an anisotropic ionosphere," Office of Telecommunications Report OT/ITS RR11, 1971. (NTIS Order No. COM 75-10939/AS).

[14] F.G. Stewart, L.A. Berry, C.M. Rush, and V. Agy, "An air-to-ground HF propagation prediction model for fast multi-circuit computation," NTIA Report 83-131, August 1983. (NTIS Order No. PB 84-145861).

[15] M. Abramowitz and LA. Stegun, *Handbook of Mathematical Functions, National Bureau of Standards AMS 55*, U.S. Government Printing Office: Washington, D.C., June 1964, pp. 297-329.

[16] J.R. Wait, "Electromagnetic surface waves," *Advances in Radio Research,* J.A. Saxton (Ed.), London:, Academic Press, 1964, pp. 157-217.

[17] V.A. Fock, *Electromagnetic Diffraction and Propagation Problems,* London: Pergamon Press, 1965.

[18] R.J. King, "Electromagnetic wave propagation over a constant impedance plane," *Radio Science* Vol. 4, No.3, pp. 225-268, March 1967.

[19] D.A. Hill and J.R. Wait, "Ground-wave attenuation function for a spherical Earth with arbitrary surface impedance," *Radio Science* Vol. 15, No.3, pp. 635-643, May-June 1980.

[20] L.A. Berry, former ITS Staff Member, Boulder, CO. (private communication, 1985).

[21] K.A. Norton, "The calculation of ground-wave field intensity over a finitely conducting spherical-Earth," Proceedings of the Institute of Radio Engineers Vol. 29, No. 12, December 1941, pp 623-639.

[22] International Telecommunications Union (ITU-R), "Ground-wave propagation curves for frequencies between 10 kHz and 10 MHz," Vol II, ITU-R Recommendation 368 (Geneva, Switzerland), 1970.

[23] J.R. Wait, "Radiation from a vertical antenna over a curved stratified ground," *National Bureau of Standards J. Res.* Vol. 56, pp. 237-244, April 1956.

[24] J.R. Wait, "On the theory of propagation of electromagnetic waves along a curved surface," *Can. J. Phys.* Vol. 36, No. l, pp. 9-17, June 1958.

[25] H. Bremmer, "Applications of operational calculus to ground-wave propagation, particularly for long waves," *IRE Trans. Ant. Prop.* AP-6, No.3, pp. 267-272, 1958.

[26] G.A. Hufford, A.G. Longley, and W.A. Kissick, "A guide to the use of the ITS irregular terrain model in the area prediction mode," NTIA Report 82-100, April 1982. (NTIS Order No. PB 82-217977).

[27] A.G. Longley and P.L. Rice, "Prediction of tropospheric radio transmission loss over irregular terrain- a computer method-1968," ESSA Tech. Report ERL 79-ITS-67, July 1968. (NTIS -Order No. AD-715-753).

[28] P.L. Rice, A.G. Longley, K.A. Norton, and A.P. Barsis, "Transmission loss predictions for tropospheric communication circuits," NBS Technical Note 101, May 1967.

[29] A.P. Barsis and P.L. Rice, "Prediction and measurement of VHF field strength over irregular terrain using low antenna heights," NBS Report 7962, January 1963.

[30] L.J. Ippolito, *Radiowave propagation in satellite communications,* New York, New York: Van Nostrand Reinhold, 1986, pp. 64-69.

[31] R.K. Crane, "Prediction of attenuation by rain," *IEEE Trans. Comm.* COM-28, No. 9, September 1980, pp. 1717-1733.

[32] E.J. Dutton, "Microwave terrestrial link rain attenuation prediction parameter analysis," NTIA Report 84-148, April 1984, (NTIS Order No. PB84-207984).

[33] P.L. Rice and N.R. Holmberg, "Cumulative time statistics of Surface-point rainfall rates," *IEEE Trans. Comm.,* Vol. COM-21, No. 10, October 1973, pp. 1131-1136.

[34] R.L. Olsen, D.V. Rogers, and D.B. Hodge, "The aRb Relation in the Calculation of Rain Attenuation," *IEEE Trans. Ant. Prop.* AP-26, No. 2, pp. 318-329, March 1978.

[35] J. Joss, J.C. Thams, and A. Waldvogel, "The Variation of Rain Drop Size Distribution at Locarno," in *Proc. Int. Congo Cl Physics,* Toronto, Canada, 1968, pp. 369-373.

[36] H.J. Liebe, "An atmospheric millimeter-wave propagation model," NTIA Report 83-137, December 1983, (NTIS Order No. PB 84-143494).

[37] H.J. Liebe, "MPM - An Atmospheric millimeter-wave propagation model," *Internat. Journal of Infrared and Millimeter Waves,* Vol. 10, No. 6, pp. 631-650, 1989.

[38] B.R. Bean and B.A. Cahoon, "A Note on the Climatic Variation of Absolute Humidity," *Bull. American Met. Soc.,* Vol. 38, No. 7, pp. 395-398, October 1957.

[39]  D.D. Crombie, "Prediction of multipath fading on terrestrial microwave links at frequencies of 11 GHz and greater," *AGARD/NATO Conf. Proc.* No. 346, 1983, Washington, D.C.

[40]  Department of Defense, *Design Handbook for Line-of-Sight Microwave Communication Systems,* MIL-HDBK-416, 1977.

# BIBLIOGRAPHIC DATA SHEET

| 1. PUBLICATION NO.<br><br>95-322 | 2. Gov't Accession No. | 3. Recipient's Accession No. |
|---|---|---|

| 4. TITLE AND SUBTITLE<br><br>Engineering Manual for the Jammer Effectiveness Model | 5. Publication Date<br><br>Sept. 1995 |
|---|---|
| | 6. Performing Organization Code<br><br>NTIA/ITS |

| 7. AUTHOR(S)<br>Nicholas DeMinco | 9. Project/Task/Work Unit No.<br><br>5 910 5534 |
|---|---|
| 8. PERFORMING ORGANIZATION NAME AND ADDRESS<br>National Telecommunications and Information Administration<br>Institute for Telecommunication Sciences<br>325 Broadway<br>Boulder, CO 80303 | |
| | 10. Contract/Grant No. |

| 11. Sponsoring Organization Name and Address | 12. Type of Report and Period Covered<br><br>NTIA Report |
|---|---|
| | 13. |

14. SUPPLEMENTARY NOTES

15. ABSTRACT *(A 200-word or less factual summary of most significant information. If document includes a significant bibliography or literature survey, mention it here.)*

This engineering manual describes a user-friendly and menu-driven computer program called the Jammer Effectiveness Model (JEM). The models used in JEM to analyze the effectiveness of a jammer in jamming a receiver/transmitter pair or network of receivers and transmitters are described. The JEM runs on personal computer in a Windows environment. The extensive design and analysis capabilities of this program have been previously limited to mainfram computers. This computer model is highly structured and modular in design, which allows for greater flexibility and expandability for future modifications.

16. Key Words *(Alphabetical order, separated by semicolons)*

jammer; jamming; propagation; communication systems models; electronic warfare; electronic countermeasures

| 17. AVAILABILITY STATEMENT<br><br>☒ UNLIMITED.<br><br>☐ FOR OFFICIAL DISTRIBUTION. | 18. Security Class. *(This report)*<br><br>Unclassified | 20. Number of pages<br><br>40 |
|---|---|---|
| | 19. Security Class. *(This page)*<br><br>Unclassified | 21. Price |